A novel soluble analog of the HIV-1 fusion cofactor, globotriaosylceramide (Gb_3), eliminates the cholesterol requirement for high affinity gp120/Gb_3 interaction

Radhia Mahfoud,* Murugesapillai Mylvaganam,† Clifford A. Lingwood,†,§ and Jacques Fantini[1],*

Institut Méditerranéen de Recherche en Nutrition,* UMR-INRA 1111, Faculté des Sciences St-Jérôme, 13397 Marseille Cedex 20, France; Research Institute,† Hospital for Sick Children, Toronto; and Departments of Biochemistry and Laboratory Medicine & Pathobiology,§ University of Toronto, Canada

Abstract **We have analyzed the interaction of adamantyl Gb_3 (adaGb_3), a semi-synthetic soluble analog of Gb_3, with HIV-1 surface envelope glycoprotein gp120. In this analog, which was orginally designed to inhibit verotoxin binding to its glycolipid receptor, Gb_3, the fatty acid chain is replaced with a rigid globular hydrocarbon frame (adamantane). Despite its solubility, adaGb_3 forms monolayers at an air-water interface. Compression isotherms of such monolayers demonstrated that the adamantane substitution resulted in a larger minimum molecular area and a more rigid, less compressible film than Gb_3. Insertion of gp120 into adaGb_3 monolayers was exponential whereas the gp120/Gb_3 interaction curve was sigmoidal with a lag phase of 40 min. Adding cholesterol into authentic Gb_3 monolayers abrogated the lag phase and increased the initial rate of interaction with gp120. This effect of cholesterol was not observed with phosphatidylcholine or sphingomyelin. In addition, verotoxin-bound adaGb_3 or Gb_3 plus cholesterol was recovered in fractions of comparable low density after ultracentrifugation through sucrose-density gradients in the presence of Triton X-100. The unique biological and physico-chemical properties of adaGb_3 suggest that this analog may be a potent soluble mimic of Gb_3, providing a novel concept for developing GSL-derived viral fusion inhibitors.**—Mahfoud, R., M. Mylvaganam, C.A. Lingwood, and J. Fantini. **A novel soluble analog of the HIV-1 fusion cofactor, globotriaosylceramide (Gb_3), eliminates the cholesterol requirement for high affinity gp120/Gb_3 interaction.** ***J. Lipid Res.*** **2002.** 43: **1670–1679.**

Supplementary key words lipid raft • microdomain • sphingolipid • infection • membrane

The involvement of cellular glycosphingolipids (GSLs) in the attachment and fusion of enveloped viruses has been recognized for a long time (1, 2). In the outer leaflet of the plasma membrane, GSLs can organize into moving platforms, or rafts, onto and into which specific proteins attach within the bilayer. Such rafts play an important role in endocytosis and signal transduction (3–5). This lateral organization probably results from preferential packing of sphingolipids and cholesterol, based on their physicochemical properties (6, 7). Consequently, sphingolipid-cholesterol rafts are insoluble in the detergent Triton X-100 at 4°C and those detergent-insoluble membranes can be purified by centrifugation on a sucrose-density gradient (3). In the present work, the term raft will be restricted to the sphingolipid/cholesterol-rich domains believed to exist in cell membranes prior to detergent treatment, since detergent-insoluble membranes and rafts are not necessarily identical (7).

Several lines of evidence support the concept that HIV-1 fusion occurs in GSLs-enriched microdomains of the plasma membrane: *i*) the CD4 receptor interacts with the monosialoganglioside GM3 and with globotriaosylceramide (Gb_3), and is accordingly localized in GSL-enriched microdomains (8–11); *ii*) the HIV-1 surface envelope glycoprotein gp120 binds to several GSLs, including GM3 and Gb_3 (10–13); *iii*) the fusion complex is assembled in GSLs-enriched microdomains (14); *iv*) removal of cellular cholesterol renders primary cells and cell lines resistant to HIV-1-mediated syncytium formation and to infection by various HIV-1 isolates (15). Moreover, GSLs are necessary to trigger the conformational changes in the envelope glycoprotein required for membrane fusion (16, 17). Among the limited number of GSLs able to promote HIV-1 fusion, Gb_3 is certainly the more potent (11, 16, 17).

Pioneer studies have shown that synthetic analogs of

Manuscript received 18 April 2002 and in revised form 4 June 2002.
DOI 10.1194/jlr.M200165-JLR200

Abbreviations: adaGb3, adamantyl Gb3; adaSGC, adamantyl-sulfatide; DPPC, dipalmitoyl-phosphatidylcholine; GSL, glycosphingolipid; PAPC, palmitoyl-arachidonoyl-phosphatidylcholine; SM, sphingomyelin.

[1] To whom correspondence should be addressed.
e-mail: jacques.fantini@univ.u-3mrs.fr

GSL could recognize HIV-1 gp120 and inhibit HIV-1 fusion (18, 19). These studies and others (20–22) have shown that the structure of the aglycone of natural and synthetic glycoconjugates can alter the affinity of the GSL-ligand interaction. Although the sugar hydroxyls and substitutions constitute the primary determinants of binding specificity, the aglycone structure may promote different intramolecular interactions, particularly at the hydrophilic sugar/hydrophobic ceramide interface (21), to influence GSL-protein interactions. Therefore, there is a crucial need for new GSL analogs with a high affinity for viral ligands (23–26). Ideally, these second generation analogs would mimic the structural organization of GSL in their membrane microdomains, and, at the same time, be sufficiently soluble in water. Since the lipid moiety of GSL is known to modulate ligand binding affinity, developing biologically active soluble GSL is a challenging task (24). Recently, a highly active derivative of Gb_3 was obtained by replacing the fatty acid chain of the GSL with adamantane, resulting in a water soluble semi-synthetic analog which retained affinity for the bacterial toxin verotoxin (27). These data prompted us to analyze the interaction of adamantyl-Gb_3 ($adaGb_3$) with HIV-1 gp120.

EXPERIMENTAL PROCEDURES

Materials

Gb_3 was purified from human red blood cells by preparative thin layer chromatography as described previously (11). When indicated, Gb_3 purified from human renal epithelium was used (27). $AdaGb_3$ was prepared from purified Gb_3 as reported (27). Adamantyl-sulfatide (adaSGC) was prepared by a similar method (28). The multibranched synthetic peptide SPC3 ($[GPGRAF]_8$-$[K]_4$-$[K]_2$-K-βA) (29) was obtained from Eurethics (Paris, France). The HIV-1 (IIIB isolate) surface envelope glycoprotein gp120 was provided by the Medical Research Council (13). Cholesterol, galactosylceramide (GalCer), sulfatide, sphingomyelin (SM), phosphatidylcholine (PC), and BSA were from Sigma.

Surface pressure measurements

The surface pressure was measured with a fully automated microtensiometer (μTROUGH SX, Kibron Inc. Helsinki, Finland). The apparatus allowed the recording of pressure-area compression isotherms and the kinetics of interaction of a ligand with the monomolecular film using a set of specially designed Teflon troughs. All experiments were carried out in a controled atmosphere at 20°C ± 1°C. Monomolecular films of Gb_3 or $adaGb_3$ (1–2 μg) were spread on pure water subphases (volume of 800 μl) from hexane/chloroform/ethanol solution as described previously (23). After spreading of the film, 5 min was allowed for solvent evaporation. To measure the interaction of HIV-1 gp120, SPC3, or BSA with glycolipid monolayers, the ligand was injected in the subphase with a 10 μl Hamilton syringe, and pressure increases produced were recorded for the indicated time. The data were analyzed with the Filmware 2.3 program (Kibron Inc. Helsinki, Finland). The accuracy of the system under our experimental conditions was ± 0.25 $mN \cdot m^{-1}$ for surface pressure.

Sucrose-density gradient ultracentrifugation

Dried samples of $adaGb_3$ (100 μg), Gb_3 (100 μg), or a mixture of Gb_3 (100 μg) and cholesterol (50 μg) were dissolved in 1.5 ml of MES-Triton buffer (pH 7.2, 1% Triton X-100). In some experiments, SM replaced the cholesterol. The solution was vortexed (1 min), sonicated (1 min), heated at 55°C (5 min), and vortexed (1 min). Then 1.5 ml 73% sucrose solution in MES (pH 7.2) was added and gently mixed and allowed to stand at room temperature for 1 h. The mixture was then layered with 2 ml of 30% sucrose containing 10 μg/ml FITC-labeled VT1B, with or without a 50 molar excess of SPC3 peptide. The tube was overlayed successively with 2 ml of 30% sucrose and 3 ml of 5% sucrose and condensed lipid species separated by floatation ultracentrifugation at 64,000 rpm for 66 h at 4°C. The tubes were photographed under UV and visible illumination. For glycolipid extraction, fractions from the sucrose gradient were applied to C18 SepPak columns, washed extensively with water, and glycolipids eluted with methanol.

Curve fitting

Experimental data were analyzed with the Origin program, version 3.5 (Microcal software). When indicated, the Boltzman (x,A1,A2,x0,dx) function producing a sigmoidal curve was used according to the equation:

$(A1-A2)/[1 + \exp((x-x0)dx)] + A2$ with parameters of x0 (center, i.e., x at y50), dx (width), A1 (Y initial), and A2 (Y final). *(Eq. 1)*

RESULTS

Physicochemical properties of Gb_3 and $adaGb_3$

The molecular structures of Gb_3 and its adamantyl derivative $adaGb_3$ are shown in **Fig. 1**. The adamantane ring structure provides a condensed, rigid, hydrophobic frame. Pressure-area isotherms of these glycolipids are shown in **Fig. 2**. Both glycolipids formed stable films. The high compressibility of Gb3 and ada-Gb3 at all film pressures and the absence of discontinuities in their isotherms show that they exist in the liquid expanded state up to film collapse. Thus, although $adaGb_3$ is highly soluble in water (up to 10 mM), it has retained the property of natural Gb_3 to form a compressible film when spread at the air-water interface. Interestingly, the collapse pressure for $adaGb_3$ (52 $mN \cdot m^{-1}$) was significantly higher than that observed for natural Gb_3 (29 $mN \cdot m^{-1}$). This indicates a higher resistance to compression of $adaGb_3$ versus Gb_3, resulting in the formation of a more rigid liquid crystalline phase. This is consistent with the finding that the minimum molecular area for $adaGb_3$ (120 $Å^2$) was larger than that of native Gb_3 (80 $Å^2$). At increasing molecular areas (>250 $Å^2$), the surface

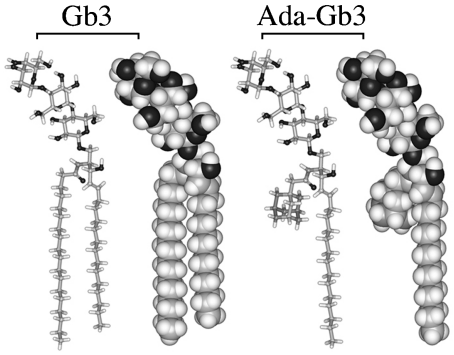

Fig. 1. Structural models of Gb_3 and adamantyl Gb3 ($adaGb_3$).

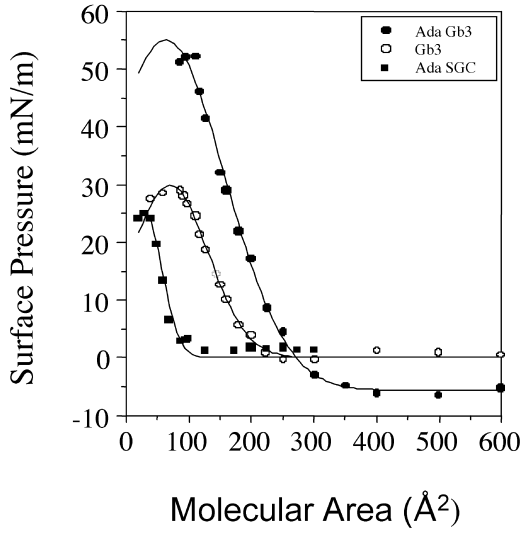

Fig. 2. Compression isotherms (pressure vs. area) of Gb_3 (open circle), adaGb3 (closed circled), and adamantyl-sulfatide (adaSGC) (square). The films were automatically compressed at a constant rate.

pressure for $adaGb_3$, but not Gb_3, falls below zero, suggesting that under these conditions, $adaGb_3$ dissolves in the aqueous subphase. This is not seen with adaSGC (28), an adamantyl derivative of sulfatide (3′-sulfo-GalCer), demonstrating that adamantane alone is not responsible for this effect (Fig. 2). Finally, the adamantyl derivative of GalCer did not form stable monolayers, showing that the adamantane substitution conferred specific physico-chemical effects in different glycolipids.

A model for the possible organization of the $adaGb_3$ monolayer as a function of surface pressure is shown in **Fig. 3**. At high surface pressure, $adaGb_3$ is confined to a minimum area of 120 Å². This is considerably greater than the molecular cross-section of $adaGb_3$, indicating that water molecules could be part of an extended structural organization of the interface. Low order aggregates of $adaGb_3$ accumulate as the surface pressure is increased and such aggregates may mimic the arrangement of Gb_3 sugars in cholesterol rich lipid microdomains. At lower surface pressures, the solubility and tendancy of $adaGb_3$ to monomerize promotes exchange into the bulk solvent to decrease the surface pressure relative to that of water. Reorientation of the sugar moiety to the monolayer interface will increase surface tension and lower surface pressure without dramatically affecting surface energy, i.e. a high surface tension monomeric $adaGb_3$ monolayer.

Interaction of HIV-1 gp120 with Gb_3 and $adaGb_3$

Gb_3 and $adaGb_3$ were spread at the air-water interface at an initial surface pressure (πi) of 11.5 $mN \cdot m^{-1}$. HIV-1 gp120 was then added in the aqueous subphase. The interaction of the viral glycoprotein with the glycolipid films was studied by surface pressure measurements. As shown in **Fig. 4A**, the insertion of gp120 into the film of natural Gb_3 occurred after an initial lag phase of 40 min. Similar data were obtained with six different batches of gp120 and Gb_3 purified from two distinct pellets of human red blood cells (mean lag phase 33.3 min, range 20–40 min, n = 12). Then the insertion reaction proceeded at an initial rate of 0.05 $mN \cdot m^{-1} \cdot min^{-1}$ and the equilibrium was reached after 135 min of incubation. A sigmoidal fit obtained with the Boltzman equation is shown (initial pressure A1, 11.62; final pressure A2, 17.71; center x0, 100.70; width dx, 18.0). In contrast, the insertion of gp120 into the film of $adaGb_3$ occurred exponentially without any lag at an initial rate of 0.8 $mN \cdot m^{-1} \cdot min^{-1}$ (Fig. 4B). In this case, the equilibrium was reached after 15 min of incubation with the viral glycoprotein. The maximal surface pressure increase ($\Delta\pi_{max}$) induced by gp120 was between 6 and 7 $mN \cdot m^{-1} \cdot min^{-1}$ for both Gb_3 and $adaGb_3$.

To assess the specificity of the gp120-glycolipid interactions, monomolecular films of Gb_3 and $adaGb_3$ were prepared at various initial pressures (πi) and the surface pressure increase induced by gp120 on these films was determined after reaching the equilibrium (**Fig. 5**). For both Gb_3 and $adaGb_3$, the compressibility of the monomolecular film was gradually decreased as the initial pressure of the monolayer increased. The influence of the initial surface pressure on the compressibility of the lipid monolayer

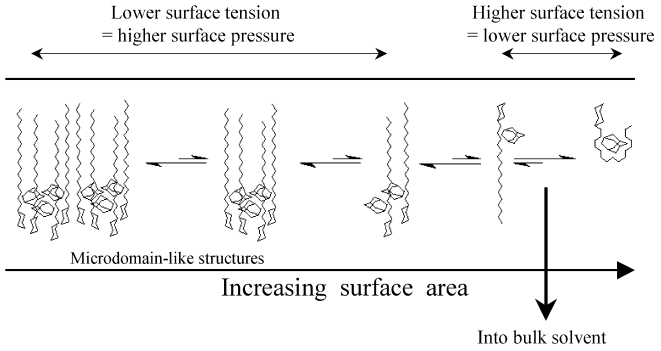

Fig. 3. Possible aggregation status of $adaGb_3$ monolayers as a function of molecular surface area. Reorientation of $adaGb_3$ at the air/water interface would explain the observed negative surface pressure at high surface areas. Low order aggregates may form condensed glycolipid structures at higher surface pressure. For clarity, some $adaGb_3$ molecules have been represented without the adamantyl ring.

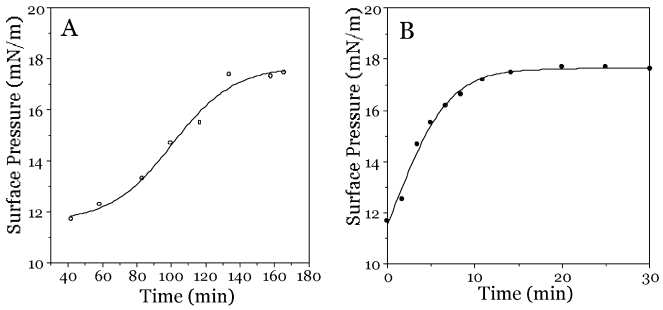

Fig. 4. Interaction of HIV-1 gp120 with a monomolecular film of Gb_3 (A) or $adaGb_3$ (B) at the air-water interface. A monolayer of Gb_3 or $adaGb_3$ was prepared at the air-water interface of a microtensiometer at an initial surface pressure (πi) of 11.5 $mN \cdot m^{-1}$. HIV-1 gp120 (50 nM) was added in the aqueous subphase underneath the monolayer and the variations in the surface pressure ($\Delta\pi$, expressed in $mN \cdot m^{-1}$) were recorded as a function of time.

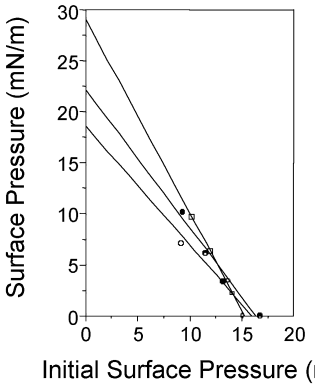

Fig. 5. Specificity of interaction between gp120 and Gb_3 or $adaGb_3$. The data show the maximal surface pressure increase ($\Delta\pi_{max}$) reached after injection of HIV-1 gp120 (50 nM) under a monomolecular film of Gb3 (open circle) or $adaGb_3$ (closed circle) at various initial surface pressures. The interaction of gp120 with Gb3 purified from human renal epithelium is also shown (square).

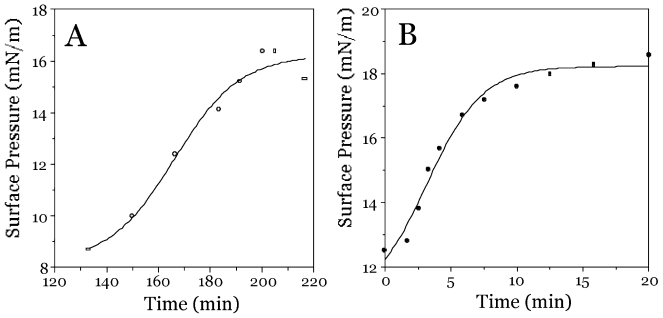

Fig. 6. Interaction of a multibranched V3 peptide with a monomolecular film of Gb_3 (A) or $adaGb_3$ (B) at the air-water interface. A monolayer of Gb_3 or $adaGb_3$ was prepared at the air-water interface of a microtensiometer at an initial surface pressure (πi) of 10–12 $mN{\cdot}m^{-1}$. The multibranched V3 peptide SPC3 (100 nM) was added in the aqueous subphase underneath the monolayer and the variations in the surface pressure ($\Delta\pi$, expressed in $mN{\cdot}m^{-1}$) were recorded as a function of time.

demonstrates the high specificity of the interaction as previously established for several other lipids and ligands (30). Similar results were obtained with another batch of Gb_3 purified from human renal epithelium (Fig. 5). However, this was not the case with adaSGC, the adamantyl derivative of sulfatide (3′-sulfo-GalCer) that interacted to the same level with gp120 at all surface pressures tested in the range of 10–15 $mN{\cdot}m^{-1}$ (data not shown). This result demonstrated that the adamantane group alone was not responsible for the specific interaction of the analog with gp120.

Involvement of the V3 loop of gp120 for the interaction with Gb_3 and $adaGb_3$

Several lines of evidence suggest the involvement of the V3 domain of gp120 in the recognition of plasma membrane GSLs. In particular, a multivalent synthetic peptide (SPC3) derived from the consensus hexamer motif GPGRAF binds to cell surface GSLs and inhibit HIV-1 fusion in various cell types (29). As shown in **Fig. 6A**, the insertion of the V3 peptide SPC3 into a monomolecular film of Gb_3 occurred after a lag phase of 150 min. The initial rate of insertion was 0.13 $mN{\cdot}m^{-1}{\cdot}min^{-1}$ and the maximal surface pressure increase ($\Delta\pi_{max}$ = 7 $mN.m^{-1}$) was observed after 200 min of incubation. A sigmoidal fit obtained with the Boltzman equation is shown (initial pressure A1, 8.21; final pressure A2, 16.23; center x0, 166.27; width dx, 12.6). In contrast, the insertion of the V3 peptide into a monomolecular film of $adaGb_3$ proceeded exponentially without any lag phase at an initial rate of 1.16 $mN{\cdot}m^{-1}{\cdot}min^{-1}$ (Fig. 6B). The equilibrium was reached after 15 min of incubation ($\Delta\pi_{max}$ = 6 $mN{\cdot}m^{-1}$). The specificity of interaction was assessed by incubating the V3 peptide with monomolecular films of Gb_3 and $adaGb_3$ at various initial surface pressures. As shown in **Fig. 7**, the decreased compressibility of the monolayers when the initial pressure increased demonstrated that the insertion of the peptide was highly specific.

Effect of cholesterol on Gb_3-gp120 interaction

Next, we investigated the effects of cholesterol, which is known to condense glycolipids in their natural plasma membrane environment (i.e., membrane rafts) (3, 4), on Gb_3-gp120 interaction. To this end, a mixed monolayer consisting of 20% cholesterol and 80% authentic Gb_3 from red blood cells (mol/mol) was prepared at the air-water interface. After stabilization of the mixed film at an initial pressure of 9.6 $mN{\cdot}m^{-1}$, gp120 (50 nM) was added in the aqueous subphase. The interaction proceeded at an initial rate of of 0.9 $mN{\cdot}m^{-1}{\cdot}min^{-1}$ without any lag phase (**Fig. 8A**). The equilibrium ($\Delta\pi_{max}$ = 5.5 $mN{\cdot}m^{-1}$) was reached after 45 min of incubation. Similar data were obtained for higher concentrations of cholesterol (molar ratio of 1:1 between Gb_3 and cholesterol), except that in this case the initial rate was 0.15 $mN{\cdot}m^{-1}{\cdot}min^{-1}$ (**Table 1**). In contrast, gp120 started to interact with a monolayer of pure Gb_3 only after 40 min of incubation, as shown in Fig. 4A. The effect of cholesterol was selective for Gb_3, since it was not observed with GalCer (Fig. 8B) or SGC (Fig. 8C). In contrast, the presence of cholesterol in a GalCer monolayer slightly reduced gp120 insertion. These data prompted

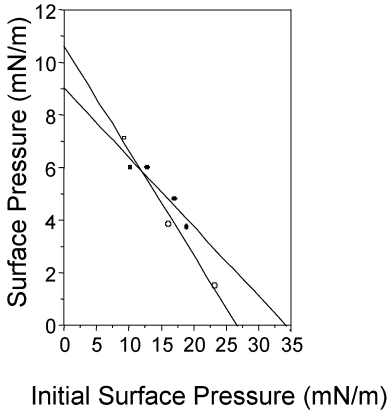

Fig. 7. Specificity of interaction between a multibranched V3 peptide and Gb_3 or $adaGb_3$. The data show the maximal surface pressure increase reached after injection of the multibranched V3 peptide (100 nM) under a monolecular film of Gb_3 (open circle) or $adaGb_3$ (closed circle) at various initial surface pressures.

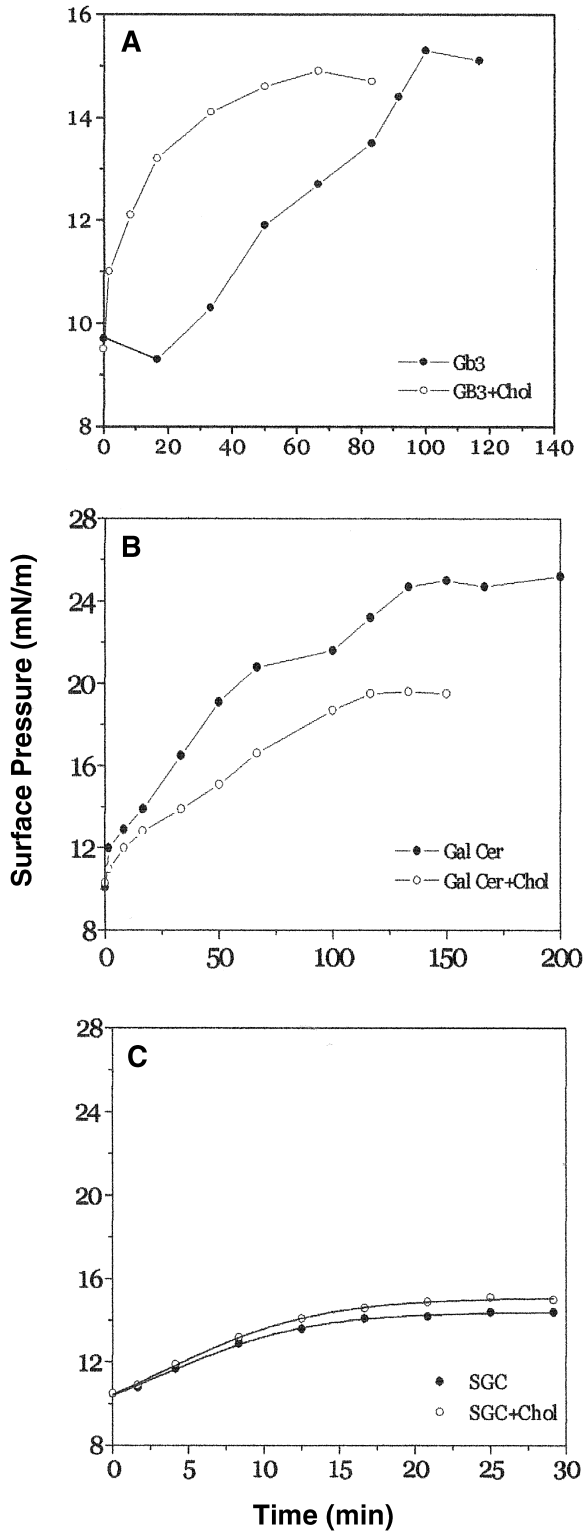

Fig. 8. Effect of cholesterol on gp120-glycosphingolipid (GSL) interactions. Monolayers of Gb_3 (A), GalCer (B), or sulfatide (C) were prepared in either the absence (closed circle) or presence (open circle) of cholesterol at an initial surface pressure (πi) of 10 $mN.m^{-1}$. For mixed monolayers, the molecular ratio was 2:8 and 1:1 for Gb_3-cholesterol and GalCer-cholesterol (mol/mol), respectively. HIV-1 gp120 (50 nM) was added in the aqueous subphase underneath the monolayer and the surface pressure was continuously recorded as a function of time.

TABLE 1. Interaction between HIV-1 gp120 and various lipid monolayers

Lipid	Lag Phase	vi	$\Delta\pi_{max}$
	min	$mN{\cdot}m^{-1}{\cdot}min^{-1}$	$mN{\cdot}m^{-1}$
Gb3	33.3	0.032	6.1
GalCer	0	0.148	14.9
SM	16.7	0.041	7.6
Gb3 + Chol (1:1)	0	0.150	5.2
Gb3 + SM (1:1)	16.7	0.041	7.6
Gb3 + Chol + SM (1:1:1)	17	0.041	6.5
GalCer + SM (1:1)	0	0.100	9.5
GalCer + Chol (1:1)	0	0.120	9.3
GalCer + Gb3 (1:1)	50	0.023	5.3
GalCer + Gb3 + Chol (1:1:1)	0	0.052	11.8

Monolayers were prepared at an initial surface pressure of 10 mN·m-1. HIV-1 gp120 (50 nM) was added in the aqueous subphase underneath the monolayer and the surface pressure was continuously recorded as a function of time. The initial rate of interaction (vi) and the maximal surface pressure increase ($\Delta\pi_{max}$) were determined with the same batch of gp120. The results are the mean of three independent determinations (SD < 15%).

us to study the interaction of gp120 with a mixed monolayer of GalCer and Gb_3 (1:1, mol/mol). Under these conditions, the interaction started after a lag phase of 50 min (initial rate of 0.023 $mN{\cdot}m^{-1}{\cdot}min^{-1}$). The addition of cholesterol in the monolayer resulted in a marked stimulation of gp120 insertion (suppression of the lag phase, initial rate of 0.052 $mN{\cdot}m^{-1}{\cdot}min^{-1}$ and higher $\Delta\pi_{max}$). These data are summarized in Table 1.

Effect of SM on monolayer Gb_3-gp120 interaction

Since SM is an important component of membrane rafts (4, 5, 7), the effect of this sphingolipid on Gb_3-gp120 interactions was also investigated. As summarized in Table 1, gp120 interacted with SM monolayers with a lag phase of 16.7 min. The rate of interaction after this initial phase was close to the one observed for pure Gb_3 (respectively 0.041 and 0.032 $mN{\cdot}m^{-1}{\cdot}min^{-1}$). Surprisingly, the same pattern of interaction was observed when gp120 was incubated with a mixed monolayer of Gb_3 and SM (1:1, mol/mol). Thus under these conditions, SM did not induce an improvement of the Gb_3-gp120 interaction as seen with cholesterol. Moreover, the stimulatory effect of cholesterol was not observed when Gb_3 was incorporated in a monolayer of SM (i.e., when gp120 was incubated with a Gb3-cholesterol-SM monolayer (1:1:1, mol/mol/mol).

In natural membranes, glycerophospholipids are also present within sphingolipid microdomains and may contribute to the binding of protein ligands to lipid rafts. For these reasons, we prepared monolayers in which the sphingolipids were embedded in palmitoyl-arachidonoyl-phosphatidylcholine (PAPC). Under the present conditions, PAPC did not improve the interaction of gp120 with Gb_3. Nevertheless, the stimulatory effect of cholesterol was still observed when Gb_3 was incorporated in a monolayer of PAPC (data not shown). Similar data were obtained when dipalmitoyl-phosphatidylcholine (DPPC) was used.

Recovery of adaGb$_3$ into Triton X-100-resistant condensed lipid structures

Since adaGb$_3$ eliminates the lag phase and cholesterol requirement for optimal gp120/Gb$_3$ interaction, we investigated whether adaGb$_3$ was able to form Triton resistant dense lipid aggregates, variously characterized as "lipid rafts," "detergent resistant microdomains," "detergent insoluble microdomains," or "glycolipid enriched microdomains," typically separated on a discontinuous sucrose ultracentrifugation gradient after cell extraction (7). To facilitate visualization of any such structures, we centrifuged the lipids though a layer of FITC-VT1B.

When adaGb$_3$ alone was centrifuged, adaGb$_3$/VT1B complexes were concentrated in a single band corresponding to a low density fraction (**Fig. 9**, lane 1), i.e., where "raft-like" structures are expected to migrate (7). In contrast, native Gb$_3$ did not form an FITC-VT1B labeled dense band (Fig. 9, lane 2). For the native glycolipid, a condensed lipid band was obtained only when Gb$_3$ was mixed with cholesterol (Fig. 9, lane 3), consistent with the results of the monolayer study. SM was less effective than cholesterol to promote condensed Gb$_3$ lipid structures, monitored under visible light but due to quenching (resulting from the basic charge?) could not be used with FITC-VT1B. In the presence of excess SPC3, FITC-VT1B binding to the adaGb$_3$ band was competed out (Fig. 9, lane 4 vs. 5). The adaGb$_3$ band was still evident under visible light (not shown).

Analysis of the Gb$_3$ content of the sucrose gradient for the Gb$_3$/cholesterol mixture confirmed the presence of Gb$_3$ within the VT1B labeled condensed lipid band (**Fig. 10A**). The Gb$_3$ content of this band was dependent on the cholesterol concentration (Fig. 10B). Inclusion of SM increased the Gb$_3$ content markedly (Fig. 10C) but VT1B binding was not increased (not shown).

Overall these data suggest that: *i*) adaGb$_3$ can spontaneously form condensed, detergent resistant aggregates as Gb$_3$ does only in the presence of cholesterol, *ii*) functionally, SM cannot substitute for cholesterol, *iii*) SM has no additive effect in terms of VT1/Gb$_3$ +cholesterol binding, and *iv*) these molecular structures are recognized by both VT1B and the multibranched V3 peptide SPC3.

Lack of interaction between BSA and adaGb$_3$

One potential drawback of synthetic soluble analogs of lipids is that they may bind to serum albumin, resulting in a total loss of biological activity in presence of serum. In order to study this possibility, monolayers of adaGb$_3$ were prepared at the air-water interface and BSA was injected in the aqueous subphase. As shown in **Fig. 11**, serum albumin did not significantly affect the surface pressure of the monomolecular film. Furthermore, when the multibranched V3 peptide SPC3 was injected in the subphase in presence of a 5-molar excess of serum albumin, its interaction with adaGb$_3$ was not affected. Thus, serum albumin did not bind to adaGb$_3$ and did not prevent the binding of adaGb$_3$ to the V3 peptide.

DISCUSSION

It is now well established that a wide variety of pathogens, including both bacteria and viruses, use GSLs as binding sites on the cell surface of host cells (1, 2, 11, 23, 31–33). Accordingly, there is a considerable interest in developing synthetic analogs of GSLs as specific inhibitors of glycolipid-pathogen interactions (24–26). The complex role played by the lipid moiety in glycolipid interactions has delayed the development of such analogs which have sufficient water solubility and, in the same time, mimic the structural and functional organization of GSLs in the

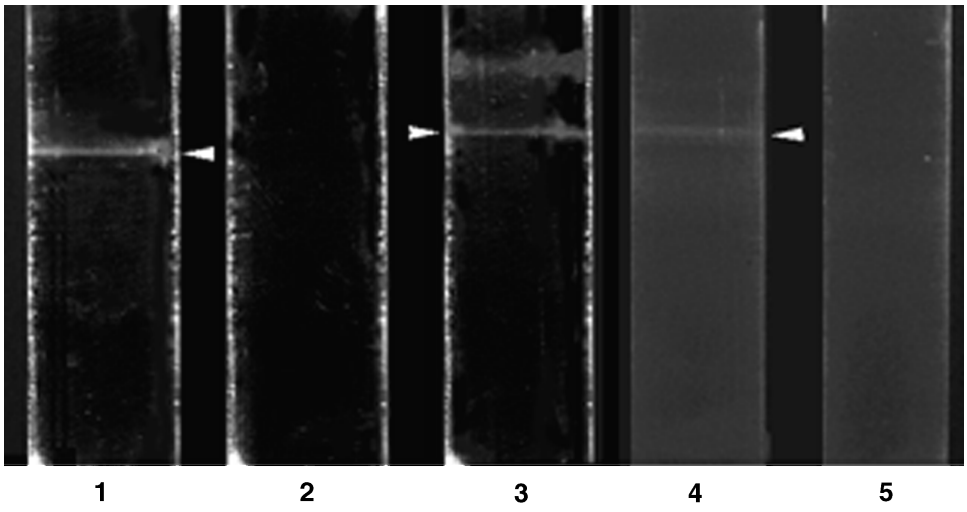

Fig. 9. Recovery of adaGb$_3$ into Triton X-100-resistant condensed lipid structures. AdaGb$_3$ (tubes 1, 4, 5), authentic Gb$_3$ (tube 2), and a mixture of authentic Gb$_3$ and cholesterol (tube 3) were submitted to sucrose gradient ultracentrifugation through a layer containing FITC-labeled VT1B alone or in the presence of a 50-fold molar excess of SPC3 peptide (tube 5). The tubes were illuminated under UV. The fluorescent labeled bands are arrowed.

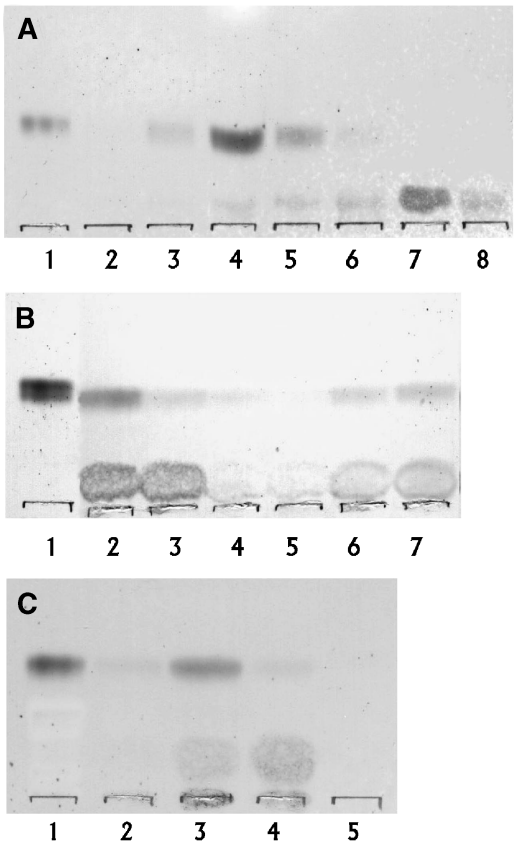

Fig. 10. Gb_3 content of condensed lipid structures. Gb_3/cholesterol/triton mixtures were subjected to discontinuous sucrose gradient ultracentrifugation as in Fig. 9 and fractions were collected and analyzed for Gb_3 content by thin layer chromatography and orcinol spray for carbohydrate. A: Gb_3/cholesterol 2:1 (μg/μg) fractionated from the top of the gradient (lanes 2–8), Lane 1 renal Gb_3 standard; lane 4 represents the fraction containing the FITC-VT1B labeled band in Fig. 9 and contains most of the Gb_3. The slower migrating species is residual sucrose. B : Gb_3-cholesterol 50:1 (μg/μg) lanes 2–4; Gb_3-cholesterol 2:1 (μg/μg) lanes 5–7. Lanes 2–4 and lanes 5–7 are the equivalent to lanes 2–4 in A. Increasing the cholesterol content increases the Gb_3 forming condensed lipid structures. C: Each lane represents the fraction containing the condensed lipid structure (A, lane 4). Lane 1 renal Gb_3 standard; lane 2 Gb_3-cholesterol 2:1 (μg/μg), lane 3 Gb_3-cholesterol-sphingomyelin (SM) 2:1:1 (μg/μg/μg), lane 4 Gb_3-cholesterol-phosphatidylcholine 2:1:1 (μg/μg/μg) lane 5 SM-cholesterol-phosphatidyl choline 1:1:1 (no band on the gradient is seen). Gb_3 within the condensed lipid structure is increased following the inclusion of SM.

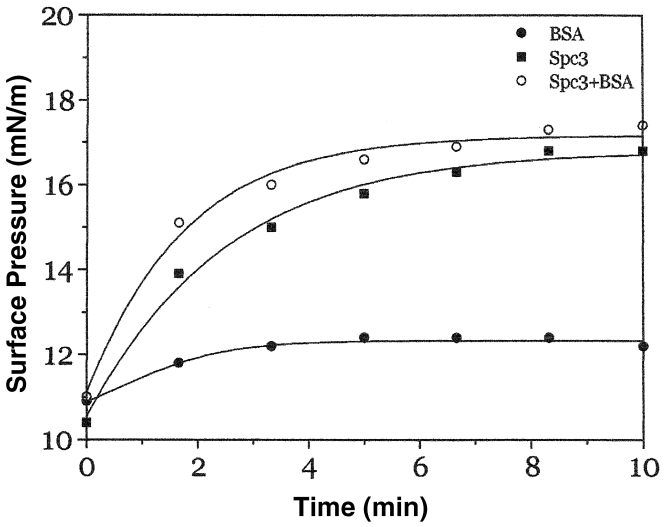

Fig. 11. Bovine serum albumin does not affect the interaction of the V3 peptide with adaGb_3. A monolayer of adaGb_3 was prepared at the air-water interface at an initial surface pressure (πi) of 10 $mN \cdot m^{-1}$. The variations in the surface pressure ($\Delta\pi$, expressed in $mN \cdot m^{-1}$) were recorded as a function of time after addition of 500 nM BSA (BSA, closed circle), 100 nM V3 peptide SPC3 (square), or a mixture of BSA + SPC3 (500 and 100 nM, respectively, open circle) in the aqueous subphase underneath the monolayer.

plasma membrane. The structure of the lipid moiety itself, particularly of the interface region, and the membrane microenvironment may play a role in the presentation of the carbohydrate for ligand binding, such that the sugar moiety alone may be without receptor activity (34). These considerations were the basis for the development of adamantyl conjugates of Gb_3 (27), the glycolipid receptor of the *Escherichia coli* derived verotoxin (32). Verotoxin/Gb_3 interaction is highly dependent on the lipid moiety of Gb_3 to present the sugar moiety for binding (22, 35). AdaGb_3 was designed as an attempt to mimic this effect in solution (27). In this class of glycolipid analogs, the fatty acid chain is replaced by rigid three-dimensional hydrocarbon frames, i.e., adamantane. The resulting adaGb_3 analog showed a markedly increased solubility in water compared with natural Gb_3, and a 1,000-fold enhanced inhibitory activity in a Gb_3-verotoxin binding assay, as compared with the free sugar (27).

Since Gb_3 is recruited by HIV-1 gp120 during the formation of the HIV-1 fusion complex involving the chemokine receptor CXCR4 (16, 36), and the GSL aglycone is crucial for gp120 binding (37), it was of great interest to analyze the interaction of gp120 with adaGb_3. Using the Langmuir film balance technology and a microtensiometer specially designed for measuring lipid-protein interactions, we found that gp120 specifically binds to adaGb_3 far more rapidly than to natural Gb_3. The analysis of Gb_3-gp120 interactions was performed with two different batches of authentic Gb_3 purified from human renal epithelium or human erythrocytes by two independent laboratories (those of J. Fantini and C. A. Lingwood), and similar results were obtained. In both cases, the insertion of gp120 into a monomolecular film of Gb_3 required a lag phase that corresponds to a binding step. Indeed, one particularity of the Langmuir method is that the surface pressure is increased only when the protein penetrates the film, resulting in the lateral moving of lipids molecules (30). The absence of lag phase during the interaction between gp120 and adaGb_3 suggests that the binding step is almost instantaneous, which is in agreement with the reported 1,000-fold enhanced affinity of verotoxin for adaGb_3 compared with the lipid free Gb_3 oligosaccharide. It was considered that the adamantane group might prevent extensive lamellar packing in aqueous systems, while duplicating in part the hydrophobic effect of the lipid moiety

on receptor function. This might explain the increased molecular area of the adaGb$_3$ as compared with Gb$_3$ (Fig. 2). The present results indicate that adaGb$_3$ excels at presenting an appropriate Gb$_3$ receptor format for gp120 recognition. The increased surface pressure at reduced molecular areas is suggestive of reduced compressibility and greater rigidity. The lag time observed for gp120/Gb$_3$ binding and the fact that the saturation binding of gp120 to Gb$_3$ and adaGb$_3$ are essentially the same, suggests that Gb$_3$ may have to undergo a lateral rearrangement, e.g., to form microdomains to efficiently bind gp120. Initially, the frequency of such domains is low but accumulate cooperatively upon gp120 binding. This cooperativity is less pronounced for the V3 domain alone (i.e., the synthetic V3 peptide) giving a longer lag phase for binding.

Moreover, the initial rate of insertion of gp120 is about 10-fold higher in the monolayer of adaGb$_3$ compared with Gb$_3$. Similar results were obtained with a synthetic V3 peptide, in agreement with previous reports demonstrating the involvement of the V3 domain of gp120 in glycolipid recognition (13, 29). Most importantly, these data show that the enhanced affinity of adaGb$_3$ for verotoxin (27) can be extrapolated to HIV-1 gp120 and a synthetic V3 peptide. Therefore, adamantyl derivatives of glycolipids provide invaluable tools for studying glycolipid receptor function. In addition, one should note that in our experimental conditions, adaGb$_3$ formed a stable monomolecular film at the air-water interface, and that gp120 insertion did not result in the collapse of the film. This suggests that the interactions between adaGb$_3$ molecules are strong enough to maintain the cohesion of the film despite the high water solubility of the analog. Hence, the experimental design used in the present study is valid for measuring the characteristics of adaGb$_3$ binding to HIV-1 gp120.

The physicochemical properties of adaGb$_3$ may explain why it exhibits such an enhanced affinity for various ligands. Similar effects are not seen with ada-SGC, indicating that the adamantane frame does not play a direct role. The fact that sulfatide is bound by gp120 (38) but adaSGC monolayers are not affected by gp120 indicates a distinction between binding and membrane fusion. This distinction was previously highlighted by the finding that increasing the cellular SGC content increased HIV binding but inhibited fusion (39). The selective role of Gb$_3$ in HIV cell fusion (16) verifies the present monolayer system as a model of this property. On the other hand, the binding of cholera toxin to GM1 only when presented as condensed complexes in artificial cholesterol/phospholipid membranes (40) is consistent with the idea that the presentation of GSLs for binding can be radically affected by the receptor density within membrane microdomains or rafts. The behavior of monomolecular films of adaGb$_3$ at the air-water interface showed that the replacement of the fatty acid chain with adamantane resulted in a more rigid monolayer with decreased compressibility (Fig. 2) despite the markedly increased water solubility of this Gb$_3$ derivative (27). This latter property likely results in the reduction of the surface pressure below that of water at increased surface areas due to the reorientation of the monomer as suggested in Fig. 3. Despite a similar minimum molecular volume, ada-SGC monolayers, unlike adaGb$_3$, were unable to resist the increased surface pressure as the surface area was reduced and collapsed. This more rigid structure may mimic the carbohydrate organization of natural Gb$_3$ in membrane rafts, as anticipated in a recent report (27). AdaSGC may not form equivalent structures. Indeed, the head group charge of sulfatide may constrain incorporation into condensed rafts, which may in turn relate to its lack of a role in HIV cell fusion (39). Consistent with this hypothesis, we observed that cholesterol, which is known to condense glycolipids in membrane rafts (5, 40), increased the initial rate of gp120 insertion in a monolayer of authentic Gb$_3$ and abrogated the lag phase. Interestingly, this effect of cholesterol was selective for Gb$_3$, since it was not observed for GalCer, or SGC, GSLs with a marked affinity for HIV-1 gp120. The lack of effect of cholesterol on gp120-GalCer interaction may be explained by the low condensing effect of cholesterol on GalCer monolayers (41). In contrast, the more bulky saccharide chain of Gb$_3$ (Fig. 1) may impair the stacking of the ceramide moiety in the monolayer, allowing the insertion of cholesterol between glycolipid molecules. This would optimize the steric presentation and recognition of the glycolipid (42), resulting in an enhanced affinity for gp120. Direct effects of cholesterol on receptor function have been reported previously (43). Another interesting finding is that gp120 interacts with mixed monolayers of GalCer and Gb$_3$, with a lag phase of 50 min. Thus in this mixture, the gp120 insertion parameters are characteristic of Gb$_3$, not GalCer. These data are in agreement with our hypothesis that the lag phase corresponds to a reorganization of the monolayer leading to an optimal presentation of the glycolipid for gp120 binding. Cholesterol stimulates this process as demonstrated by the rapid and efficient interaction observed between gp120 and a GalCer/Gb$_3$/cholesterol film (Table 1). It is possible that the high cholesterol content of the plasma membrane as opposed to the endomembrane system plays a modulatory role in relative gp120-glycolipid recognition during the HIV infectious cycle. Finally, although abundantly expressed in lipid rafts, SM (SM) does not seem to affect the presentation of Gb$_3$, since its presence in the monolayer did not improve gp120 binding (Table 1). SM did increase the Gb$_3$ content of the dense fraction of the sucrose gradient consistent with a Gb$_3$/SM interaction characteristic of lipid rafts (7), but VT1B binding was not increased (SM quenched FITC-VT1B which therefore could not be used). However, this fraction contained larger aggregates limiting interpretation. SM via interaction with cholesterol (44) may alter the Gb$_3$ domain organization when spread together at the interface. In the sucrose gradients, Gb$_3$ found in the condensed lipid fraction in the presence of cholesterol was increased several-fold by inclusion of SM but VT1B binding was not increased, suggesting that Gb$_3$-SM dense complexes are formed but not bound by VT1B. The interaction of gp120 with various mixtures of Gb$_3$, GalCer, SM, and cholesterol was not affected by the presence of PC (either PAPC or DPPC) in the reconstituted monolayers and PC had no effect on the Gb$_3$ content of cholesterol containing

Triton resistant condensed structures on a sucrose gradient. Taken together, these data strongly suggest that cholesterol (and no other lipid species) is required for optimal binding of gp120 to Gb_3 microdomains. This is in agreement with the recent demonstration that the formation of "raft domains" within reconstituted membranes critically depends on the cholesterol content (40) and that host membrane cholesterol is required for cellular infection by HIV-1 (15).

These conclusions are also supported by the sucrose ultracentrifugation studies. In solution, Gb_3 formed Triton X-100 resistant low-density condensed lipid structures when mixed with cholesterol, but not alone. In contrast, adaGb_3 could form similar structures alone, which strongly supports the view that this analog may mimic the typical organization of Gb_3/cholesterol complexes in detergent-insoluble microdomains. In such microdomains, the presentation of the Gb_3 carbohydrate may, due to changes in the interface, be optimal for gp120 binding and subsequent insertion, similar to cholera toxin/GM1 binding (40). We propose that this effect is mimicked by adaGb_3.

One important issue raised by the present study is the specificity of interaction between Gb_3/ada Gb_3 and HIV-1 gp120. Indeed, gp120 also interacts with GalCer and sulfatide (39). However, the adamantyl derivative of GalCer could not form stable monolayers at the air-water interface, whereas adaSGC, which could form monolayers (Fig. 2), was not recognized by gp120 (Fig. 8C). Thus, among the adamantyl derivatives of GSL receptors for HIV-1 gp120, adaGb_3 has unique physico-chemical and binding properties. GM1 have been shown to inhibit HIV-1 infectivity in vitro, but the action of this ganglioside was to prevent cell surface expression of CD4 (45). Indeed, the interaction of gp120 with GM1 is very weak compared with GalCer or Gb_3 (11). Moreover, subsequent addition of fetal calf serum or bovine and human serum albumin blocked GM1 action on CD4 expression, most likely through the formation of ganglioside-albumin complexes (45). For these reasons, we tested the potential effect of serum albumin on adaGb_3 monolayers. We found that BSA did not bind to adaGb_3 and did not affect the interaction of the gp120 V3 peptide with adaGb_3.

In conclusion, the results of the present study showed that semi-synthetic analogs of GSLs like adaGb_3 may functionally mimic Gb_3 microdomains, providing a new class of molecular tools for studying the role of glycolipids and lipid rafts in HIV-1 fusion (46, 47) and other biological processes (32). To the best of our knowledge, our study presents the first experimental evidence that condensed lipid structures can be formed in absence of cholesterol by a synthetic analog of a glycolipid receptor. From a therapeutic point of view, disrupting gp120-glycolipid interactions by such glycolipid derivatives would obviate the problem of resistance mutants selected by current antiretroviral treatments (48, 49) and may open a new route for controlling HIV-1 replication in infected individuals (24).

This work was supported by Canadian Institutes of Health research grant no. MT13073 (C.A.L).

REFERENCES

1. Haywood, A. M. 1994. Virus receptors: binding, adhesion strengthening, and changes in viral structure. *J. Virol.* **68:** 1–5.
2. Karlsson, K. A. 1995. Microbial recognition of target-cell glycoconjugates. *Curr. Opin. Struct. Biol.* **5:** 622–635.
3. Brown, R. E., and J. Rose. 1992. Sorting of GPI-anchored proteins to glycolipid-enriched membrane subdomains during transport to the apical cell surface. *Cell.* **68:** 533–544.
4. Simons, K., and E. Ikonen. 1997. Functional rafts in cell membranes. *Nature.* **387:** 569–572.
5. Brown, R. E. 1998. Sphingolipid organization in biomembranes: what physical studies of model membranes reveal. *J. Cell Sci.* **111:** 1–9.
6. Thompson, T. E., and T. W. Tillack. 1985. Organization of glycosphingolipids in bilayers and plasma membranes of mammalian cells. *Annu. Rev. Biophys. Biophys. Chem.* **14:** 361–386.
7. London, E., and D. A. Brown. 2000. Insolubility of lipids in triton X-100: physical origin and relationship to sphingolipid/cholesterol membrane domains (rafts). *Biochim. Biophys. Acta.* **1508:** 182–195.
8. Sorice, M., I. Parolini, T. Sansolini, T. Garofalo, V. Dolo, M. Sargiacomo, T. Tai, C. Peschle, M. R., Torrisi, and A. Pavan. 1997. Evidence for the existence of ganglioside-enriched plasma membrane domains in human peripheral lymphocytes. *J. Lipid Res.* **38:** 969–980.
9. Millan, J., J. Cerny, V. Horejsi, and M. A. Alonso. 1999. CD4 segregates into specific detergent-resistant T-cell membrane microdomains. *Tissue Antigens.* **53:** 33–40.
10. Hammache, D., N. Yahi, G. Piéroni, F. Ariasi, C. Tamalet, and J. Fantini. 1998. Sequential interaction of CD4 and HIV-1 gp120 with a reconstituted membrane patch of ganglioside GM3: implications for the role of glycolipids as potential HIV-1 fusion cofactors. *Biochem. Biophys. Res. Commun.* **246:** 117–122.
11. Hammache, D., N. Yahi, M. Maresca, G. Piéroni, and J. Fantini. 1999. Human erythrocyte glycosphingolipids as alternative cofactors for human immunodeficiency virus type 1 (HIV-1) entry: evidence for CD4-induced interactions between HIV-1 gp120 and reconstituted membrane microdomains of glycosphingolipids (Gb3 and GM3). *J. Virol.* **73:** 5244–5248.
12. Fantini, J., D. G. Cook, N. Nathanson, S. L. Spitalnik, and F. Gonzalez-Scarano. 1993. Infection of colonic epithelial cell lines by type 1 human immunodeficiency virus is associated with cell surface expression of galactosylceramide, a potential alternative gp120 receptor. *Proc. Natl. Acad. Sci. USA.* **90:** 2700–2704.
13. Hammache, D., G. Piéroni, N. Yahi, O. Delézay, N. Koch, H. Lafont, C. Tamalet, and J. Fantini. 1998. Specific interaction of HIV-1 and HIV-2 surface envelope glycoproteins with monolayers of galactosylceramide and ganglioside GM3. *J. Biol. Chem.* **273:** 5967–5971.
14. Manes, S., G. del Real, R. A. Lacalle, P. Lucas, C. Gomez-Mouton, S. Sanchez-Palomino, R. Delgado, J. Alcami, E. Mira, and C. Martinez-A. 2000. Membrane raft microdomains mediate lateral assemblies required for HIV-1 infection. *EMBO Rep.* **1:** 190–196.
15. Liao, Z., L. M. Cimakasky, D. H. Nguyen, and J. E. Hildreth. 2001. Lipid rafts and HIV pathogenesis: host membrane cholesterol is required for infection by HIV type 1. *AIDS Res. Hum. Retroviruses.* **17:** 1009–1019.
16. Puri, A., P. Hug, K. Jernigan, J. Barchi, H. Y. Kim, J. Hamilton, J. Wiles, G. J. Murray, R. O. Brady, and R. Blumenthal. 1998. The neutral glycosphingolipid globotriaosylceramide promotes fusion mediated by a CD4-dependent CXCR4-utilizing HIV type 1 envelope glycoprotein. *Proc. Natl. Acad. Sci. USA.* **95:** 14435–14440.
17. Hug, P., H. M. Lin, T. Korte, X. Xiao, D. S. Dimitrov, J. M. Wang, A. Puri, and R. Blumenthal. 2000. Glycosphingolipids promote entry of a broad range of human immunodeficiency virus type 1 isolates into cell lines expressing CD4, CXCR4, and/or CCR5. *J. Virol.* **74:** 6377–6385.
18. Fantini, J., D. Hammache, O. Delézay, N. Yahi, C. André-Barrès, I. Rico-Lattes, and A. Lattes. 1997. Synthetic soluble analogs of galactosylceramide (GalCer) bind to the V3 domain of HIV-1 gp120 and inhibit HIV-1-induced fusion and entry. *J. Biol. Chem.* **272:** 7245–7252.
19. Faroux-Corlay, B., L. Clary, C. Gadras, D. Hammache, J. Greiner, C. Santaella, A. M. Aubertin, P. Vierling, and J. Fantini. 2000. Synthesis of single- and double-chain fluorocarbon and hydrocarbon

galactosyl amphiphiles and their anti-HIV-1 activity. *Carbohydr. Res.* **327:** 223–260.
20. Jones, D. H., C. A. Lingwood, K. R. Barber, and C. W. M. Grant. 1997. Globoside as a membrane receptor: a consideration of oligosaccharide communication with the hydrophobic domain. *Biochemistry.* **36:** 8539–8547.
21. Mamelak, D., M. Mylvaganam, E. Whetstone, E. Hartmann, W. Lennarz, P. Wyrick, J. Raulston, H. Han, P. Hoffman, and C. A. Lingwood. 2001. Hsp70s contain a specific sulfogalactolipid binding site. Differential aglycone influence on sulfogalactosyl ceramide binding by recombinant prokaryotic and eukaryotic hsp70 family members. *Biochemistry.* **40:** 3572–3582.
22. Boyd, B., G. Magnusson, Z. Zhiuyan, and C. A. Lingwood. 1994. Lipid modulation of glycolipid receptor function. Availability of Gal(alpha 1–4)Gal disaccharide for verotoxin binding in natural and synthetic glycolipids. *Eur. J. Biochem.* **223:** 873–878.
23. Fantini, J., D. Hammache, G. Piéroni, and N. Yahi. 2000. Role of glycosphingolipid microdomains in CD4-dependent HIV-1 fusion. *Glycoconj. J.* **17:** 199–204.
24. Fantini, J. 2000. Synthetic soluble analogs of glycolipids for studies of virus-glycolipid interactions. *Methods Enzymol.* **311:** 627–638.
25. Yarema, K. J., and C. R. Bertozzi. 1998. Chemical approaches to glycobiology and emerging carbohydrate-based therapeutic agents. *Curr. Opin. Chem. Biol.* **2:** 49–61.
26. Weber, K. T., D. Hammache, J. Fantini, and B. Ganem. 2000. Synthesis of glycolipid analogues that disrupt binding of HIV-1 gp120 to galactosylceramide. *Bioorg. Med. Chem. Lett.* **10:** 1011–1014.
27. Mylvaganam, M., and C. A. Lingwood. 1999. Adamantyl globotriaosyl ceramide: a monovalent soluble mimic which inhibits verotoxin binding to its glycolipid receptor. *Biochem. Biophys. Res. Commun.* **257:** 391–394.
28. Mamelak, D., M. Mylvaganam, E. Tanahashi, H. Ito, H. Ishida, M. Kiso, and C. A. Lingwood. 2001. The aglycone of sulfogalactolipids can alter the sulfate ester substitution position required for hsc70 recognition. *Carbohydr. Res.* **335:** 91–100.
29. Delézay, O., D. Hammache, J. Fantini, and N. Yahi. 1996. SPC3, a V3 loop-derived synthetic peptide inhibitor of HIV-1 infection, binds to cell surface glycosphingolipids. *Biochemistry.* **35:** 15663–15671.
30. Maggio, B. 1994. The surface behavior of glycosphingolipids in biomembranes: a new frontier of molecular ecology. *Prog. Biophys. Mol. Biol.* **62:** 55–117.
31. Lingwood, C. A. 1998. Oligosaccharide receptors for bacteria: a view to a kill. *Curr. Opin. Cell Biol.* **2:** 695–700.
32. Lingwood, C. A. 1999. Glycolipid receptors for verotoxin and Helicobacter pylori: role in pathology. *Biochim. Biophys. Acta.* **1455:** 375–386.
33. Fantini, J., M. Maresca, D. Hammache, N. Yahi, and O. Delézay. 2000. Glycosphingolipid (GSL) microdomains as attachment platforms for host pathogens and their toxins on intestinal epithelial cells: activation of signal transduction pathways and perturbations of intestinal absorption and secretion. *Glycoconj. J.* **17:** 173–179.
34. Lingwood, C. A. 1996. Aglycone modulation of glycolipid receptor function. *Glycoconj. J.* **13:** 495–503.
35. Kiarash, A., B. Boyd, and C. A. Lingwood. 1994. Glycosphingolipid receptor function is modified by fatty acid content. Verotoxin 1 and verotoxin 2c preferentially recognize different globotriaosyl ceramide fatty acid homologues. *J. Biol. Chem.* **269:** 11138–11146.
36. Puri, A., P. Hug, K. Jernigan, P. Rose, and R. Blumenthal. 1999. Role of glycosphingolipids in HIV-1 entry: requirement of globotriosylceramide (Gb3) in CD4/CXCR4-dependent fusion. *Biosci. Rep.* **19:** 317–325.
37. Mylvaganam, M., and C. A. Lingwood. 1999. A convenient oxidation of natural glycosphingolipids to their "ceramide acids" for neoglycoconjugation. Bovine serum albumin-glycosylceramide acid conjugates as investigative probes for HIV gp120 coat protein-glycosphingolipid interactions. *J. Biol. Chem.* **274:** 20725–20732.
38. Gadella, B. M., D. Hammache, G. Piéroni, B. Colenbrander, L. M. G. van Golde, and J. Fantini. 1998. Glycolipids as potential binding sites for HIV: topology in the sperm plasma membrane in relation to the regulation of membrane fusion. *J. Reprod. Immunol.* **41:** 233–253.
39. Fantini, J., D. Hamache, O. Delézay, G. Piéroni, C. Tamalet, and J. Fantini. 1998. Sulfatide inhibits HIV-1 entry into CD4-/CXCR4+ cells. *Virology.* **246:** 211–220.
40. Radhakrishnan, A., T. G. Anderson, and H. M. McConnell. 2000. Condensed complexes, rafts, and the chemical activity of cholesterol in membranes. *Proc. Natl. Acad. Sci. USA.* **97:** 12422–12427.
41. Ali, S., J. M. Smaby, H. L. Brockman, and R. E. Brown. 1994. Cholesterol's interfacial interactions with galactosylceramides. *Biochemistry.* **33:** 2900–2906.
42. Nyholm, P. G., and I. Pasher. 1993. Steric presentation and recognition of the saccharide chains of glycolipids at the cell surface: favoured conformations of the saccharide-lipid linkage calculated using molecular mechanics (MM3). *Int. J. Biol. Macromol.* **15:** 43–51.
43. Gimpl, G., K. Burger, and F. Fahrenholz. 1997. Cholesterol as modulator of receptor function. *Biochemistry.* **36:** 10959–10974.
44. Slotte, J. P. 1999. Sphingomyelin-cholesterol interactions in biological and model membranes. *Chem. Phys. Lipids.* **102:** 13–27.
45. Chieco-Bianchi, L., M. L. Calabro, M. Panozzo, A. De Rossi, A. Amadori, L. Callegaro, and A. Siccardi. 1989. CD4 modulation and inhibition of HIV-1 infectivity induced by monosialoganglioside GM1 in vitro. *AIDS.* **3:** 501–507.
46. Kozak, S. L., J. M. Heard., D. Kabat. 2002. Segregation of CD4 and CXCR4 into distinct lipid microdomains in T lymphocytes suggests a mechanism for membrane destabilization by human immunodeficiency virus. *J. Virol.* **76:** 1802–15.
47. Popik, W., T. M. Alce, and W. C. Au. 2002. Human immunodeficiency virus Type 1 uses lipid raft-colocalized CD4 and chemokine receptors for productive entry into $CD4^+$ T Cells. *J. Virol.* **76:** 4709–22.
48. Yahi, N., C. Tamalet, C. Tourrès, N. Tivoli, F. Volot, J. A. Gastaut, H. Gallais, J. Moreau, and J. Fantini. 1999. Mutation patterns of the reverse transcriptase and protease genes in human immunodeficiency virus type 1-infected patients undergoing combination therapy: survey of 787 sequences. *J. Clin. Microbiol.* **37:** 4099–4106.
49. Tamalet, C., N. Yahi, C. Tourrès, P. Colson, A. M. Quinson, C. Dhiver, and J. Fantini. 2000. Multidrug resistance genotypes (insertions in the beta3-beta4 finger subdomain and MDR mutations) of HIV-1 reverse transcriptase from extensively treated patients: incidence and association with other resistance mutations. *Virology.* **270:** 310–316.